Richard Wardle* and Ian Simmonds
University of Melbourne,
Victoria, Australia

1. INTRODUCTION

A picture of the mid-Holocene (6,000 years before present) climate has been built using many well dated proxy records. These reconstructions of the so-called 'Climatic Optimum' indicate a climate that differs from that of today, both regionally and seasonally. Understanding of the causes of the observed changes can be furthered through the comparison of General Circulation Model (GCM) simulations with the aforementioned palaeo reconstructions. This study employs the Melbourne University GCM (MUGCM) to elucidate the global atmospheric dynamics during this period of Earth's history. We examine any differences in the Australian climate, both in its mean signatures and the transient systems it experiences, within the context of a global simulation. We also attempt, for the first time, to elucidate the development and intensification of tropical and extratropical cyclones during this epoch, using a state-of-the-art vortex tracking scheme (Simmonds and Murray, 1999, Simmonds *et al.* 1999).

2. MODELLING METHODOLOGY

The MUGCM is a spectral model, using a rhomboidal truncation at wavenumber 21. This gives a grid resolution of 3.25^o lat and 5.625^o lon for the physical parameterizations. In the vertical, the σ-coordinate is used with 9 discrete levels. A semi-Lagrangian advection scheme of water vapour is used which yields an improved hydrological cycle. For complete description of the model set-up see Noone and Simmonds, 2002.

Two MUGCM simulation data sets have been used in the present study, both covering 100 years. The first data set is a present day (PD) numerical simulation which successfully replicates the distribution and variability of extratropical cyclone activity as well as the main features of winds, temperatures, and precipitation of the mean circulation. The climatology of an earlier version of the model is more completely described in Simmonds *et al.* 1988, among others. The second data set is the model simulated climate of the mid-Holocene (MH). The palaeo simulation is compared to the PD run and statistical significance of the responses to the prescribed changes are estimated, enabling separation of the signal from the noise that is inherent in the model.

The prescribed surface boundary conditions of orography, coastlines and sea surface temperatures are consistent with the Paleoclimate Modelling Intercomparison Project (PMIP) with only the solar radiation and atmospheric CO_2 concentrations differing in the MH run from that of the PD simulation. Hence, this work determines the sensitivity to a change in radiative forcing of the atmosphere. The reduced MH atmospheric CO_2 levels are 280 ppmv compared with 330 ppmv for the PD. The incoming solar radiation for each simulation is computed according to the method of Berger, 1978 and the insolation anomaly between the two epochs, which results from changes in the Earth's orbital parameters, is shown in Figure 1.

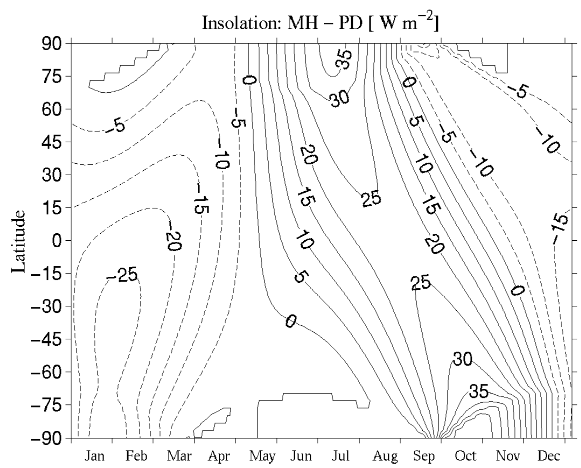

Figure 1: The annual cycle of the difference in the insolation at the top of the atmosphere between the mid-Holocene (MH) and present day (PD) simulations. Solid (dashed) lines indicate positive (negative) anomalies during MH. The contour interval is 5 W m^{-2}.

The solar radiation anomaly pattern displays enhanced seasonality in the northern hemisphere with positive (negative) radiation anomalies in the northern summer (winter). This is contrast to the insolation anomaly south of the equator, where the positive inso-

*Corresponding author address: Richard Wardle, School of Earth Sciences, University of Melbourne, Victoria, Australia, 3010. email: rwardle@unimelb.edu.au

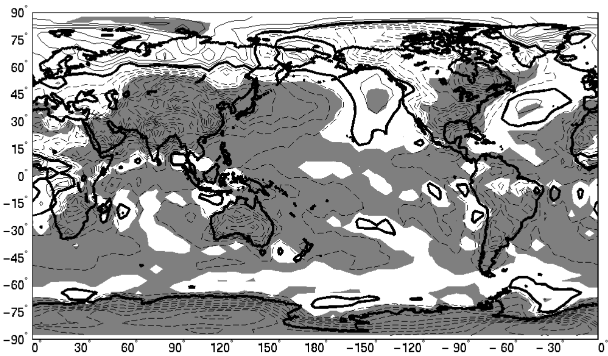

(a) DJF Surface air temperature anomaly (^{o}C)

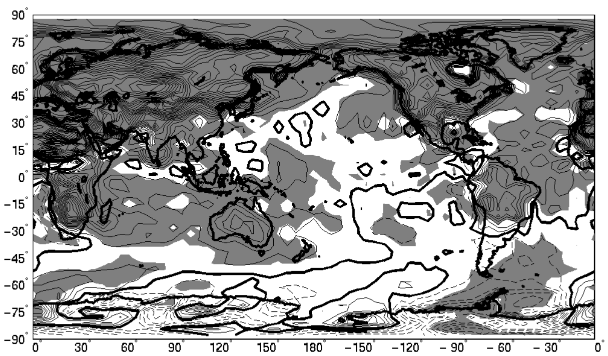

(b) JJA Surface air temperature anomaly (^{o}C)

Figure 2: The difference in the surface temperature between the MH and PD simulations in (a) DJF and (b) JJA. The contour interval is 0.1 ^{o}C. Solid (dashed) lines indicate positive (negative) anomalies during MH. Regions of statistical significance at the 95 % confidence level are shaded.

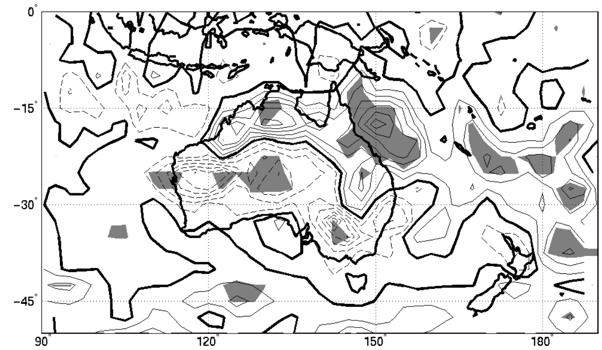

(a) DJF cyclone system density anomaly ((deg lat)$^{-2}$)

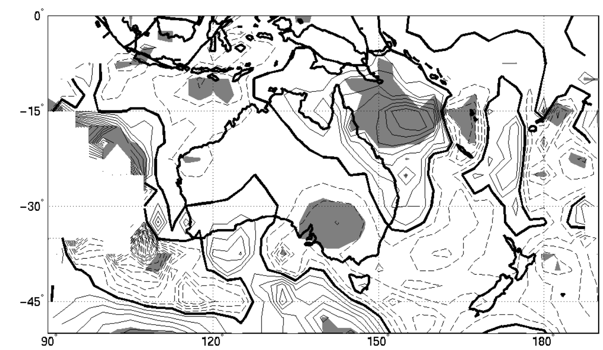

(b) DJF Laplacian of pressure anomaly (hPa (deg lat)$^{-2}$)

Figure 3: The DJF difference between the MH and PD (a) cyclone system density ((deg lat)$^{-2}$) and (b) the mean Laplacian of pressure calculated at the center of each cyclone (hPa (deg lat)$^{-2}$). The contour intervals are (a) 0.1×10^{-3} (deg lat)$^{-2}$ and (b) 0.01 hPa (deg lat)$^{-2}$. Solid (dashed) lines indicate positive (negative) anomalies during MH. Regions of statistical significance at the 95 % confidence level are shaded.

lation anomaly occurs in austral spring (SON) with a rapid transition to a negative anomaly in the southern summer (DJF).

3. RESULTS

Figure 2 shows that the mid-Holocene simulation produces a weaker surface temperature seasonal cycle in the Southern Hemisphere, in contrast to the modelled enhanced seasonality in the Northern Hemisphere. Relative to PD, Australian surface air temperatures are lower during the southern hemisphere summer (DJF) and are higher during its winter (JJA), consistent with the radiation anomaly pattern shown in Figure 1.

As a result, there is a reduction in the strength of the summer monsoon and its associated precipitation for northern Australia. However, the reduction in rainfall directly associated with the monsoon in the north is more than offset by enhanced summer precipitation associated with a greater number of tropical cyclones in the simulation (Figure 3a). The enhanced numbers of tropical cyclones are also more intense, as measured through the use of the mean Laplacian of the pressure field calculated at the center of a system (Figure 3b). In the southern region of the continent the number of extratropical cyclones is unchanged except in spring, during which relatively more systems result in higher precipitation rates over the interior of Australia. However, we have found that the winter cyclones on the southern Australian coast are less intense and, as a result, lower rainfall amounts are seen compared to PD.

In general, Australia experiences less precipitation during each season with the exception of spring. A

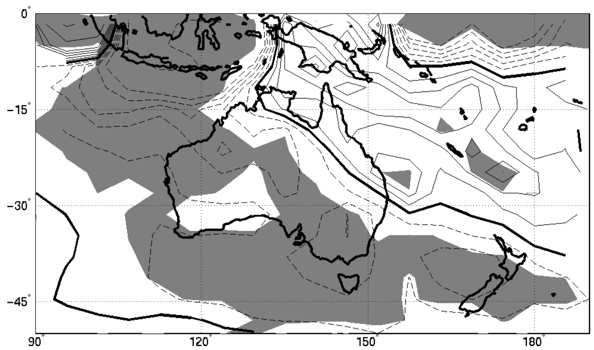

(a) Annual precipitation anomaly (mm day^{-1})

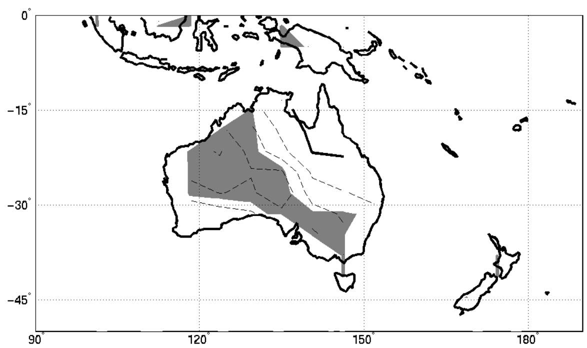

(b) Annual soil moisture anomaly (cm)

Figure 4: The difference in the annual mean (a) precipitation and (b) soil moisture content between the MH and PD simulations. Positive (negative) MH anomalies are solid (dashed). The contour interval are (a) $\pm$ [0.1 .2 .3 .4 .5 1. 2. 3. 4 5 6 7 8 9 10 12 14 16] mm day^{-1} and (b) 0.25 cm. Regions of statistical significance at the 95 % confidence level are shaded.

consequence of the precipitation response, integrated over a year (Figure 4a), is that the modelled Australian surface moisture content is drier than today (Figure 4b). In contrast, NE Queensland, a location of many palaeo records [for example, Moss and Kershaw, 2000], is wetter, due to the enhanced precipitation of the region averaged over an annual cycle.

Palynological proxy studies [e.g. Kershaw *et al.*, 2000] suggest that during the mid-Holocene the Australian continent was generally warmer during winter and the summer was cooler than today. The model is able to reproduce a response to the radiative forcing that is consistent with the palaeo data. However, the model is at variance with all proxy records with a drier MH continent, suggesting that the consequences of potentially important feedbacks, such as ocean temperature, need to be investigated further or that the palaeo record needs to be revisited.

4. REFERENCES

Kershaw A.P., Quilty P.G., David B., Van Huet S. and McMinn A., 2000: Paleobiogeography of the Quaternary of Australia. *Memoir of the Association of Australasian Palaeontologists*, **23**, 471-516.

Moss, P.T., and A.P. Kershaw, 2000: The last glacial cycle from the humid tropics of northeastern Australia: comparison of a terrestrial and a marine record. *Palaeogeography, Palaeoclimatology, Palaeoecology*, **155**,155-176.

Noone, D., and I. Simmonds, 2002: Associations between δ^{18}O of water and climate parameters in a simulation of atmospheric circulation for 1979-95. it J. Climate, **15**, 3150-3169.

Simmonds, I., and R.J., Murray, 1999: Southern extratropical cyclone behaviour in ECMWF analyses during the FROST special observing periods. *Wea. Forecasting*, **14**, 878-891.

Simmonds, I., R.J., Murray, and R.M. Leighton, 1999: A refinement of cyclone tracking methods with data from FROST. *Aust. Meteor. Mag.*, Special Issue, 35-49.

Simmonds, I., G. Trigg, and R. Law, 1988: The climatology of the Melbourne University General Circulation Model, *Tech. Rep.* **31**.